Plasmonics
DOI 10.1007/s11468-016-0357-4

Dielectric Dispersion in Ga_2S_3 Thin Films

S. R. Alharbi[1] · **A. F. Qasrawi**[2]

Received: 4 July 2016 / Accepted: 8 August 2016

Abstract In this work, the structural, compositional, optical, and dielectric properties of Ga_2S_3 thin films are investigated by means of X-ray diffraction, scanning electron microscopy, energy dispersion X-ray analysis, and ultraviolet—visible light spectrophotometry. The Ga_2S_3 thin films which exhibited amorphous nature in its as grown form are observed to be generally composed of 40.7 % Ga and 59.3 % S atomic content. The direct allowed transitions optical energy bandgap is found to be 2.96 eV. On the other hand, the modeling of the dielectric spectra in the frequency range of 270–1,000 THz, using the modified Drude-Lorentz model for electron-plasmon interactions revealed the electrons scattering time as 1.8 (*fs*), the electron bounded plasma frequency as ~0.76–0.94 (*GHz*) and the reduced resonant frequency as 2.20–4.60 $\times 10^{15}$ (*Hz*) in the range of 270–753 THz. The corresponding drift mobility of electrons to the terahertz oscillating incident electric field is found to be 7.91 (cm^2/Vs). The values are promising as they nominate the Ga_2S_3 thin films as effective candidates in thin-film transistor and gas sensing technologies.

Keywords Gallium sulfide · Optical materials · Coating · Dielectric properties · Plasmon

✉ A. F. Qasrawi
atef.qasrawi@atilim.edu.tr; atef.qasrawi@aauj.edu

[1] Physics Department, Faculty of Science- Al Faisaliah, King Abdulaziz University, Jeddah, Saudi Arabia

[2] Groups of Physics at AAUJ and at Faculty of Engineering, Atilim University, 06836 Ankara, Turkey

Introduction

One of the materials that has recently attracted attention as a smart optoelectronic component is the Ga_2S_3 compound. The monoclinic Ga_2S_3 crystal is reported to exhibit a second harmonic generation feature [1]. With this property, the crystal is employed for nonlinear optical conversions. In another work, a defect-related red and green emission at 1.62 and 2.24 eV, respectively, was observed from the Ga_2S_3 films. Both of the colors are reported to be sensitive to the conjunction with GaAs [2] indicating that the *p*-Ga_2S_3/*n*-GaAs heterostructures are of great potential in sensor applications for high-power lasers. Moreover, the Sn doped β-Ga_2O_3 nanowires which were deposited onto Si(001) substrates exhibited photoluminescence at 2.7 eV. The red shift of the emission was tunable from 2.7 to 1.8 eV. The tuning was done via postgrowth processing under H_2S atmosphere above 500 °C. The Si/Ga_2S_3 heterojunction behaved as a solar cell with power conversion efficiency of 8.3 % [3]. Furthermore, ultrafast pump-probe and transient photoluminescence spectroscopy studies on β-Ga_2O_3/Ga_2S_3 nanowires displayed two emission lines; one is broad blue emission with a lifetime of 2.4 ns originating from the β-Ga_2O_3 and another is red emission centered at 680 nm with a lifetime of 19 μs [4].

On the other hand, nonlinear optical analysis on the Ga_2S_3 revealed possibilities of using this material for terahertz applications [5]. The nonlinear optical frequency conversion monoclinic Ga_2S_3 crystal is observed to provide a second-harmonic generator and an optical parametric oscillator [6]. In addition, the related studies have shown that the bulky Ga_2S_3 can be a strong potential competitor to a layered GaSe and its solid solutions which are possessing novel outstanding optical properties [7–9]. For this reason here in this work, we aim to explore the structural and optical properties of the Ga_2S_3 in thin film form. Besides the general optical

Published online: 17 August 2016

properties, the work will particularly focus on the analysis and modeling of the dielectric spectra in the frequency range of 270–1,000 THz. The main physical parameters needed for direct optical applications are computed from the correlation between the experimentally measured and theoretically modeled dielectric spectra.

Experimental Details

The Ga_2S_3 thin films are prepared by the evaporation of the high purity Ga_2S_3 powders (Alfa Aeser). Tungsten boats were used for source evaporation. The substrate was ultrasonically cleaned glass. The growth was actualized under a vacuum pressure of 10^{-5} mbar. The film's thickness (0.93 μm) was controlled by a thickness controller attached to the VCM Norm 600 thin film evaporator. The obtained 22 × 22 mm^2 samples were studied by means of scanning electron microscopy using a Joel JSM 7600F instrument that has an energy dispersion X-ray (EDX) analyzer and Ultima IV X-ray diffraction system (Cu Kα = 1.54178°A). The optical transmittance and reflectance spectra were recorded with the help of an evolution 300 spectrophotometer that is equipped with VEEMAX II reflectometer.

Results and Discussion

The X-ray diffraction results of the Ga_2S_3 thin films which are deposited onto glass substrates are shown in Fig. 1a. As the figure shows, no intensive peaks were observed indicating that the as-grown films are of amorphous nature. For more deep structural analysis, the as-grown films were subjected to a scanning electron microscopic imaging with magnification of 60,000. The SEM image which appears in Fig. 1b displays very intensive distribution of grains. The grain size and distribution looks better in Fig. 1c which represented the 120,000 magnification of 7.0 mm scanned area of the film. The latter image indicates that the grains are randomly distributed with an average size of ~50 nm. The random distribution of the grains confirms the amorphous nature of the films [8].

On the other hand, the energy dispersion X-ray spectroscopy (EDXA) analysis on different regions of the films revealed homogenous distribution of elements through the films. The EDXA data displayed an atomic content percentage of 40.7 % Ga and 59.3 % S which represent the correct stoichiometry of the Ga_2S_3 compound. In general, most of the as-grown thin films which were tested over different preparation cycles (one cycle includes 22 × 22 mm2 nine samples) exhibited the correct stoichiometry. However, some samples which are located far (~5–6 cm) from the substrates center, in addition to the Ga_2S_3 phase, they displayed an atomic content of 47.3 % Ga and 52.7 % S and 49.4 % Ga and 50.6 % of S. The latter values indicate the existence of the GaS phase through the films. The importance of the stoichiometry deviations lay in the idea that the films may exhibit *n*-type or *p*-type conduction when they are S or Ga rich, respectively. Studies on similar materials like GaSe have shown that the excess Se ($-2e$) in the composition causes *n*-type conduction. Similarly, excess Ga in the films caused *p*-type conduction [9]. For our samples in its worst composition, the films which were tested by the hot probe technique remained of *n*-type conduction.

The Ga_2S_3 compound is reported [10] to exist in three main polytype phases. They are known as monoclinic α -Ga_2S_3, hexagonal β -Ga_2S_3 and cubic γ-Ga_2S_3. The α -Ga_2S_3 modification exhibits wurtzite type of lattice parameters, a =

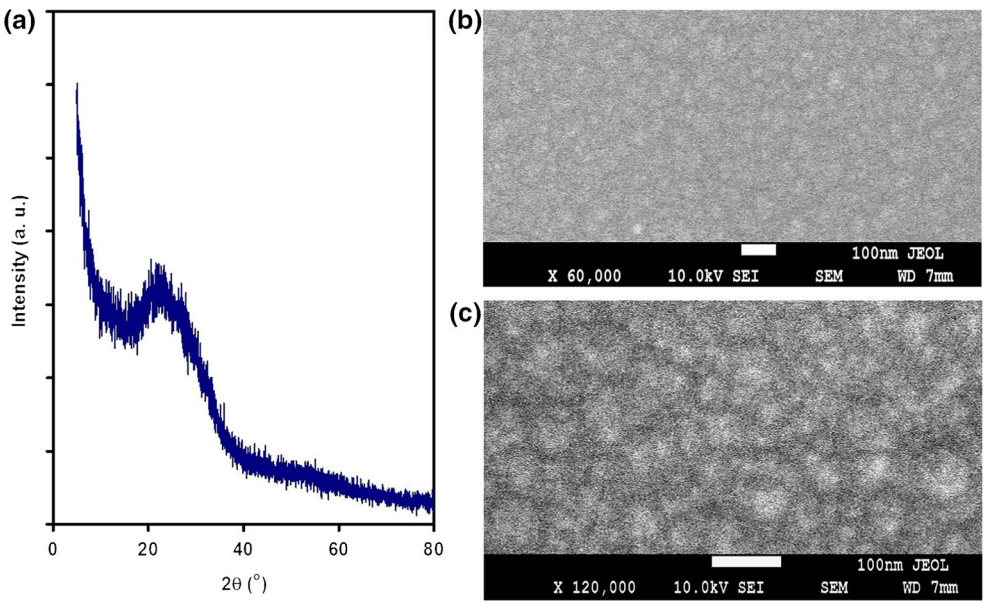

Fig. 1 **a** The X-ray diffraction patterns and the SEM images being recorded at 10 KV for a sample of 7 mm width magnified **b** 60,000 times, and **c** 120,000 times for the Ga_2S_3 thin films

11.094, $b = 9.5778$, $c = 6.395^{o}A$ and $\gamma = 141^{0\prime}15^{\prime}$, with ordered vacancies. The β -Ga_2S_3 modification exhibits wurtzite type of lattice parameters, $a = 3.6785$, $c = 6.0166^{o}A$ with disordered vacancies. In addition, the γ -Ga_2S_3 modification exhibits a zincblende type of structure that has lattice parameter of $A = 5.17^{o}A$. The latter modification type is also known to include highly disordered vacancies. The existence of these polytypes in the same film could be a main reason of the amorphous nature of the as-grown films. It also explains the nonstoichiometric behavior of some of the samples [10].

Figure 2 illustrates the optical transmittance (T), reflectance (R) and absorbance ($A = 100 - T - R$) of the Ga_2S_3 thin films being recorded in the spectral range of 350–1100 nm. Generally, the Ga_2S_3 films are highly transparent. The T value reaches 91 % at 652 nm (1.91 eV). Both of the transmittance and reflectance contained interference patterns as the incident light of wavelength (λ) exceeds 466 nm (2.67 eV). The reason for the appearance of the interference patterns in the optical spectra is mostly assigned to the constructive and destructive interference between the incident and reflected waves at the film's surface [8, 9]

The absorbance ($A = \alpha d$, d: is the film thickness) data are employed to reveal an information about the energy bandgap (E_g) of the Ga_2S_3 thin films through the relation, $(\alpha E)^2 \propto (E - E_g)$. The absorption coefficient (α)- incident photon energy (E) dependence of the Ga_2S_3 thin films in accordance with this equation (displayed in Fig. 2b) reveals a direct allowed transitions energy bandgap of 2.96 eV. This value is lower than the energy bandgap being 3.44 eV [10–12] which is reported for the monoclinic α-Ga_2S_3, it is also larger than 2.48 eV [10] which is reported for the hexagonal β–Ga_2S_3. The value 2.96 eV is in agreement with that reported for cubic γ– Ga_2S_3 [11, 12]. It is also consistent with that reported as 3.0 eV for the p-type Ga_2S_3 films which were prepared by the sulfurization of the n-type GaAs (111) surface at elevated temperatures [2].

It is also worth notifying that, the analysis of the derivative Lorentzian line-shape fits of the PTR spectra (polarized-thermoreflectance) on Ga_2S_3 revealed three energy band transitions known as $E_A = 3.052$ eV, $E_B = 3.240$ eV, and $E_{C1} = 3.328$ eV at 300 K [12]. These band-edge transitions E_A, E_B, and E_{C1} are accepted to be coming from different origins. In addition to that, an asymmetric valence-band top may have accounted for the observed optical-anisotropic effects of the monoclinic Ga_2S_3. For the α– Ga_2S_3 the highest valence band is composed of mainly S (*3p*) and some Ga (*4p*) orbitals. These *p*-states are observed to exhibit a strongly axial dependent distribution. On the opposite side, the lowest conduction-band portion of Ga_2S_3, are mainly composed of Ga (*4 s*) and a some of the *S (3p)* with distribution of density of states over a rage of 1.7–3.4 eV [12].

To give significance for the interference patterns which appeared in the reflectance spectra, the effective, real, and imaginary parts of dielectric constant were calculated using the previously described methods of calculation [9]. The resulting real (ε_r) and imaginary (ε_{im}) parts of the dielectric spectra are displayed in Fig. 3a, b, respectively. The real part of the dielectric constant exhibited very strong resonance peaks. The resonance peaks correspond to incident photon energies of 3.47, 2.96, 2.30, and 1.32 eV. The peaks, respectively, correspond to 852, 721, 570, and 330 THz. While the 2.96 eV resonating peak is clearly assigned to direct allowed transitions from the valence to the conduction band of the Ga_2S_3, in accordance with the literature data [10–12], the peaks

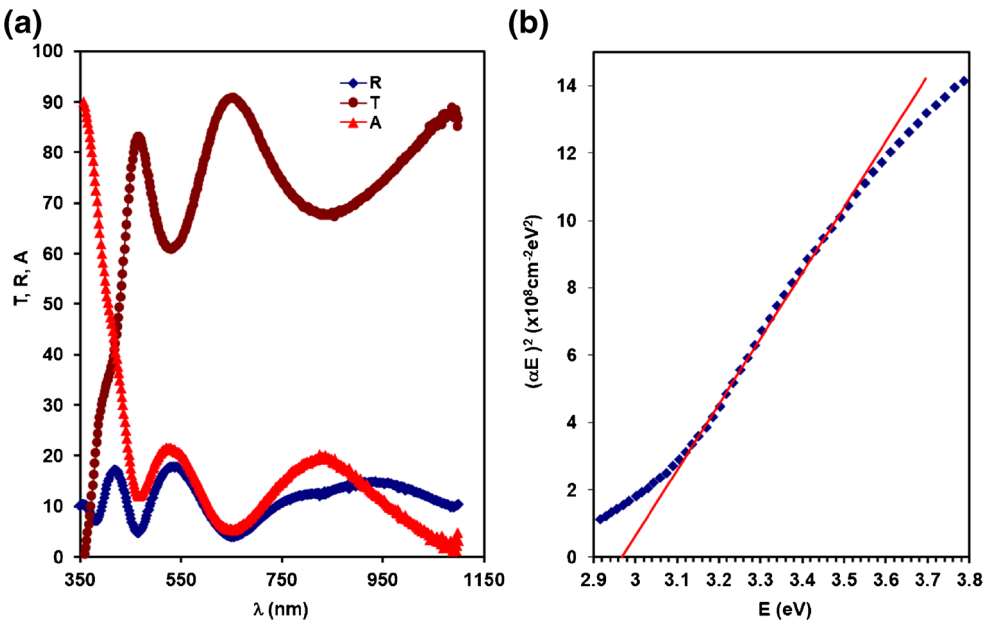

Fig. 2 **a** The transmittance, reflectance, and absorbance spectra, and **b** the $(\alpha E)^2$ -E dependence for the Ga_2S_3 thin films

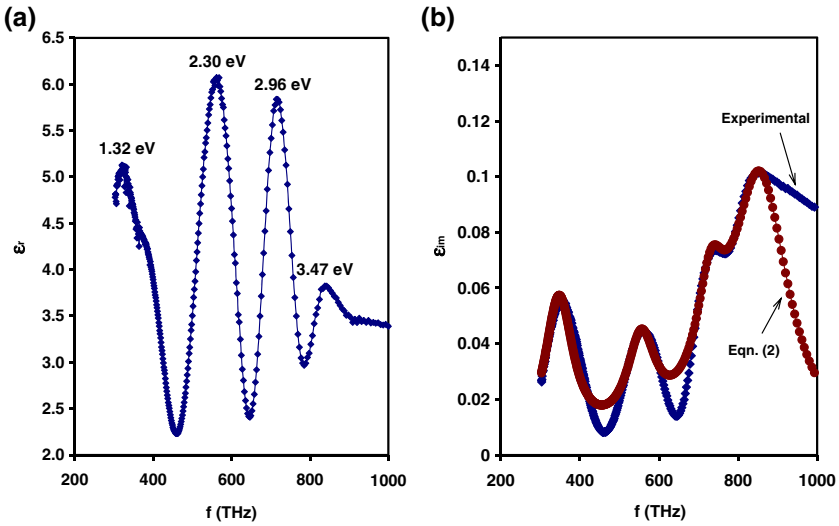

Fig. 3 **a** The real part of the dielectric spectra and **b** the imaginary part of the dielectric constant

which appeared at 3.47 eV and at 2.30 eV should correspond to the transitions in the α -and β– Ga_2S_3 polytypes, respectively. As mentioned above, the photonic transitions in the α and β -type modifications are reported to be through energy bandgaps of 3.44 and 2.48 eV, respectively [10]. The observed resonance peak at 1.32 eV is mostly assigned to the interband transitions through the energy bands of the Ga_2S_3 films. As we have discussed in the structural part, the Ga_2S_3 films exhibit amorphous nature of structure. This nominates it to exhibit high degree of surface defects. The interfacial defects are reported to easily form on the *c*-plane along *a*-axis [12]. The defects which are detected by the photoluminescence spectra are assigned to Ga and S vacancies.

The imaginary part of the dielectric constant which is shown in Fig. 3b exhibits two orders of magnitude lower values that of real one. It exhibits four resonating peaks centered at 341 (1.41 eV), 543 (2.25 eV), 735 (3.04 eV), and 842 THz (3.49 eV). The reason for the existing of these resonating peaks which in turn provide information about the optical and electrical conduction parameters could be understood from the modeling of the ε_{im}. In accordance with the Lorentz model which connects the imaginary part of the dielectric constant to the incident light frequency by the relation [13],

$$\varepsilon_{\mathrm{im}} = \frac{w_{\mathrm{pe}}^2 w}{\tau\left(\left(w_{\mathrm{e}}^2 - w^2\right)^2 + w^2\tau^{-2}\right)} \tag{1}$$

In this equation, τ, $w_{\mathrm{pe}} = \sqrt{4\pi ne^2/m^*}$ and w_{e} are the electrons scattering time, the electron bounded plasma frequency, and w_{e} is the reduced resonant frequency. *n* is the free electron density. Equation 1 can also be employed to evaluate the frequency independent drift mobility, $\mu = e\tau/m^*$ with m^* being the effective mass of free electrons. This equation provides information about the values of τ, w_{pe}, w_e and μ for single resonating peak of the dielectric constant. For coupled resonance like that which appear in Fig. 3b, the exact solution was obtained through the programming of the equation assuming generalized form of Lorentz model (known as Lorentz-Drude model). The model describes electronic interband transitions by assuming that electrons in the material are bound to the ionic atomic core and oscillate about it. The model uses *k* oscillators at major critical points in the joint density of states which correspond to interband transitions energies $\hbar w_{\mathrm{k}}$, with some additional oscillators to connect absorption between critical joints. Particularly, here in this work, we have assumed that the imaginary part of the dielectric spectra could be reproduced through the modified relation,

$$\varepsilon_{\mathrm{im}} = \sum_{i=1}^{k} \frac{w_{\mathrm{pe_i}}^2 w}{\tau_i\left(\left(w_{\mathrm{e_i}}^2 - w^2\right)^2 + w^2\tau_{\mathrm{i}}^{-2}\right)} \tag{2}$$

In this equation *k* is the number of observed peaks and the subscript *i* refers to the relative peak. For the $\varepsilon_{\mathrm{im}}$ spectra which appears in Fig. 3b, $k = 4$. The experimental data was reproduced by substituting $m^* = 0.40m_{\mathrm{o}}$ and the values of τ_{i}, $w_{\mathrm{e_i}}$ and *n* which are tabulated in Table 1 into Eq. (2). The complete solution that is obtained with the help of Eq. (2) and which is presented by the brown-colored line in Fig. 3b

Table 1 The computed parameters of the plasmon-electron interactions in the Ga_2S_3 thin films

i	$\tau_{\mathrm{i}}(fs)$	$w_{\mathrm{ei}}(\times 10^{15}\ Hz)$	$n\ (\times 10^{17}\ cm^{-3})$	$\mu\ (cm^2/Vs)$	$w_{\mathrm{pei}}\ (GHz)$
1	1.8	2.20	6.5	7.91	0.76
2	1.8	3.50	6.5	7.91	0.76
3	1.8	4.60	10.0	7.91	0.94
4	0.90	5.40	58.0	3.96	2.26

indicated a typical coupled oscillator that is subjected to damping forces of damping constant $\gamma = \tau^{-1}$. The tabulated data suggests that, the scattering time for the first three peaks (341 (1.41 eV), 543 (2.25 eV), and 735 (3.04 eV)) is the same leading to an electron drift mobility of 7.91 (cm^2/Vs). Thus, these three oscillators are subjected to the same damping force. However, the resulting reduced resonant frequency (w_e) which takes into account the effects of the local fields (interband transitions) on the dielectric function continuously increases with increasing incident light frequency. On the other hand, the electron bounded plasma frequency (w_{pe}) which depends on the number of free electrons (n), exhibits value of 0.76 *(GHz)* for the first two oscillators only. As the incident electric field frequency approaches 735 THz (third peak), the number of free electrons increases to 1.0×10^{18} (cm^{-3}) causing an increase in the value of w_{pe} to 0.94 (*GHz*). Further increase in the value of the incident field frequency to 842 THz (3.49 eV) significantly decreases the scattering time of the electrons and as a result the drift mobility falls to 3.96 (cm^2/Vs). This fall is associated with remarkable increase in the electron bounded plasma frequency (2.26 (*GHz*))) and is also ascribed to the increase in the damping coefficient γ.

Recalling that the plasmonic gas sensors are optical sensors which get benefit from the localized surface plasmons or extended surface plasmons as transducing platform and because the surface plasmons are very sensitive to dielectric variations of the environment or to electron exchange, the tabulated optical parameters that are obtained from the dielectric spectra nominate the Ga_2S_3 films as a promising device for gas sensing [14, 15]. In addition, the values of the free carrier density and drift mobility are of acceptable range of thin film transistor technology.

Conclusions

In this article, we have discussed the growth and optical characterizations of the Ga_2S_3 thin films. While the structural analysis revealed disordered nature of films, the energy dispersive X-ray analysis has shown that the Ga_2S_3 layer rarely contained GaS phase. The analysis of the optical properties allowed determining the energy bandgap. The remarkable interesting features of these films are observed in the dielectric spectra which displayed high-frequency oscillator characteristics at terahertz frequencies. The modeling of the dielectric spectra allowed determining the physical parameters of this film as a cavity for coupled oscillations. Particularly, with the plasmon frequencies of 0.76–2.26 GHz, microwave propagations through the films are controlled. The values of the computed parameters including the drift mobility, nominate the Ga_2S_3 crystals for use in communication technology owing to their optoelectronic behavior. In addition, the electron-plasmon interactions in the films suggest the applicability of these films in gas sensing technology.

Acknowledgments This project was funded by the Deanship of Scientific Research (DSR), King Abdulaziz University, Jaddah, under the grant number G-236-363-37. The authors, therefore, acknowledge with thanks the DSR technical and financial support.

References

1. Zhang M, Guo G, Zeng H, Jiang X, Fan Y, Liu B (2014a) U.S. Patent Application No. 14/565,133
2. Liu HF, Antwi KA, Yakovlev NL, Tan HR, Ong LT, Chua SJ, Chi DZ (2014a) Synthesis and phase evolutions in layered structure of Ga2S3 semiconductor thin films on epiready GaAs (111) substrates. ACS Appl Mater Interfaces 6(5):3501–3507. doi:10.1021/am4056535
3. Zervos M, Othonos A, Gianneta V, Travlos A, Nassiopoulou AG (2015) Sn doped β-Ga2O3 and β-Ga2S3 nanowires with red emission for solar energy spectral shifting. J Appl Phys 118(19):194302. doi:10.1063/1.4935633
4. Othonos KM, Zervos M, Christofides C, Othonos A (2015) Ultrafast spectroscopy and red emission from β-Ga2O3/β-Ga2S3 nanowires. Nanoscale Res Lett 10(1):1–7. doi:10.1186/s11671-015-1016-y
5. Huang, Z, Huang, JG, Kokh, KA, Svetlichnyi, VA, Shabalina, AV, Andreev, YM, Lanskii, GV (2015) Ga2S 3: Optical properties and perspectives for THz applications. In 2015 40th International Conference on Infrared, Millimeter, and Terahertz waves (IRMMW-THz) (pp. 1–2). IEEE. DOI: 10.1109/IRMMW-THz.2015.7327440
6. Zhang M, Guo G, Zeng H, Jiang X, Fan Y, Liu B (2014b) optical parametric oscillator and second harmonic generator using monoclinic phase ga2s3 crystal. U.S. Patent Application 14/565,133.
7. Caraman I, Rusu D, Ardeleanu E, Evtodiev I (2015) The detectors of uv and x radiation based on ga2s3 and gase semiconductors intercalated with Cd. Journal of Optoelectronics and Biomedical Materials 7(1):27–32
8. Kayed TS, Qasrawi AF, Elsayed KA (2016) Band offsets and optical conduction in the CdSe/GaSe interface. Curr Appl Phys 16(7):772–776. doi:10.1016/j.cap.2016.04.010
9. Qasrawi AF, Khanfar HK, Kmail RR (2016) Optical conduction in amorphous GaSe thin films. Optik-International Journal for Light and Electron Optics 127(13):5193–5195. doi:10.1016/j.ijleo.2016.03.021
10. Madelung O (2012) Semiconductors: data handbook. Springer Science & Business Media, Berlin. doi:10.1007/978-3-642-18865-7
11. Liu HF, Antwi KA, Chua CS, Huang J, Chua SJ, Chi DZ (2014b) Epitaxial synthesis, band offset, and photoelectrochemical properties of cubic Ga2S3 thin films on GaAs (111) substrates. ECS Solid State Letters 3(11):P131–P135. doi:10.1149/2.0021411ssl
12. Ho CH, Chen HH (2014) Optically decomposed near-band-edge structure and excitonic transitions in Ga2S3. Scientific reports 4(8):6143. doi:10.1038/srep06143
13. Dresselhaus M (1980) Optical properties of solids. American Scientific Publishers, New York
14. Han Z, Lin P, Singh V, Kimerling L, Hu J, Richardson K, Agarwal A, Tan DTH (2016) On-chip mid-infrared gas detection using chalcogenide glass waveguide. Appl Phys Lett 108(14):141106. doi:10.1063/1.4945667
15. Gaspera ED, Martucci A (2015) Sol-gel thin films for plasmonic gas sensors. Sensors 15(7):16910–16928. doi:10.3390/s150716910